Available online at www.sciencedirect.com
ScienceDirect
International Journal of Thermal Sciences 46 (2007) 823–833
International Journal of Thermal Sciences
www.elsevier.com/locate/ijts

Performance prediction of steam ejector using computational fluid dynamics: Part 2. Flow structure of a steam ejector influenced by operating pressures and geometries

T. Sriveerakul, S. Aphornratana *, K. Chunnanond

Sirindhorn International Institute of Technology, Thammasat University, PO Box 22 Thammasat Rangsit Post Office, Pathumthani 12121, Thailand

Received 22 March 2006; received in revised form 24 October 2006; accepted 24 October 2006

Available online 27 November 2006

Abstract

The aim of this study is to reveal the complication of the flow and the mixing process of a steam ejector used in a jet refrigeration cycle by using the simulation software package (FLUENT). In Part 1 of this work, the CFD results of the steam ejector's performance were validated with the experimental values. After the validation is satisfied, this paper is able to analyze the flow phenomena inside the steam ejector when its operating conditions and geometries were varied. Using the applications provided by the CFD software, the flow structure of the modeled ejectors could be created graphically, and the phenomena inside the flow passage were explored. The CFD method was evaluated as an efficient tool to represent the flow inside a steam ejector.

Keywords: Ejector; Jet refrigeration; Flow visualization; CFD

1. Introduction

Steam jet refrigeration is a refrigeration system that uses water as its working fluid. It utilizes a low temperature thermal energy (100–200 °C) from inexpensive or even free sources such as industrial wasted heat or a solar collector. A major component that makes the system usable is a steam ejector. It is recognized that the performance of the system depends greatly on the performance of the ejector. Hence, in order to improve the performance of an ejector, understanding of the flow inside the ejector is needed.

In this study, Computational Fluid Dynamics (CFD) was used to analyze the flow phenomena inside a steam ejector. According to the validation of the static pressure profile along the wall of the ejector, entrainment ratio, and critical back pressure as was done previously in the first part [1], it was concluded that the CFD model can efficiently represent the flow inside the steam ejector. This paper, which is the second part of the study, concentrates on the use of CFD in visualizing the change in the flow structure and the mixing process inside the steam ejector as influenced by interested parameters, ejector's operating conditions and geometries. Using the post processing available in the CFD software, the created contours of Mach number and the calculated pressure distribution at any point of interest, the flow structure and the mixing process within a steam ejector can be clearly explained. Consequently, it is believed that, with the CFD software, the better understanding of the flow within the ejector could help to improve the design of the ejector.

2. Flow and mixing process of the steam ejector

Before investigating the change in flow structure of the steam ejector influenced by interested parameters using CFD visualization, detailed explanation of the simulated flow structure is provided. Fig. 1 illustrates the contours lines of Mach number and static pressure distribution of the steam ejector when it operates at the choked flow mode.

As the high-temperature and high-pressure primary fluid enters the convergent section of the primary nozzle, the subsonic motive flow accelerates to sonic value and chokes at the nozzle

* Corresponding author. Tel.: (+662) 986 9009 ext 2210; fax: (+662) 9869009 ext 2201.
E-mail address: satha@siit.tu.ac.th (S. Aphornratana).

1290-0729/$ – see front matter
doi:10.1016/j.ijthermalsci.2006.10.012

Nomenclature

d	diameter of constant area throat	mm
l	throat length	mm
P	pressure	mbar
Rm	entrainment ratio	
T	temperature	°C
X	primary nozzle throat's diameter	mm
Y	primary nozzle exit's diameter	mm
Z	mixing chamber inlet's diameter	mm

Subscripts

C	downstream fluid
P	primary fluid
S	secondary fluid

Abbreviation

NXP	nozzle exit position

throat (1). In the divergent portion of the nozzle, the primary fluid accelerates and expands further to achieve a supersonic speed.

At the nozzle exit plane (2), it is found that the supersonic primary stream leaves the primary nozzle with its static pressure greater than that in the mixing chamber. Therefore, it is capable of additional expansion and acceleration as an "*under-expanded*" wave [2] with some value of the "*expansion angle*". To preserve the static pressure across the free boundary between the primary jet core (3) and the surrounded fluid, the first series of oblique shock and expansion waves, called the "*diamond wave*" pattern (4), is induced. This phenomenon can be investigated from the fluctuation of static pressure at the center line of the ejector while the flow passes through a mixing chamber (Fig. 1(b)).

The occurrence of a diamond wave jet core in the mixing chamber indicates the semi-separation between the high speed primary flow and the surrounded secondary fluid. Thus, the converging duct (5) for entraining a secondary fluid into the mixing chamber, similar to that was proposed by Munday and Bagster [3], is formed. Moreover, according to the large velocity difference between these two streams, the shear stress layer (6) interfacing between them is presented. The shear mixing of two streams begins as the secondary fluid is entrained and interfaces with the expanded wave. Flowing through the converging duct, the shear mixing process causes the secondary fluid to accelerate, conversely, the shear mixing and the viscosity of the fluid cause the diamond wave to decay. As investigated in Fig. 1(b), the static pressure of the flow steadily decreases at the beginning of the flow process, and the violence of the diamond wave reduces, respectively.

At the throat of the mixing chamber, most of the entrained secondary fluid accelerates and reaches the sonic velocity. Very small amounts move slightly faster than the sonic value when it flows close to the shear stress layer, but slower when it flows close to the wall boundary layer. Moreover, it is seen that the violence of the diamond wave reduces as the primary jet core travels with lower supersonic speed, consequently, a relatively smooth jet core results. Therefore, the secondary flow can be considered as choked. The choke area or "*effective area*" [3] of the secondary fluid can be estimated from the annulus area between the wall of an ejector throat and the primary fluid jet core. Despite using the CFD visualization, it is difficult to locate the exact position of the effective area within the ejector. During the choke flow mode, the entrainment ratios remained constant, the effective area, hence, can be estimated at anywhere within the constant area ejector's throat.

At a certain distance into the ejector throat or in the beginning of the diffuser section, called the "*shocking position*" (7), a non-uniform stream produces the second series of oblique shock waves (8). Therefore, when the flow is dominated by a series of oblique shocks, the static pressure gradually recovers to discharge value and the flow speed gradually decreases to subsonic level, while it passes through the diffuser, Fig. 1(b). In addition, across this process, the mixed stream loses most of its total pressure. However, in concept, a series of oblique shock should provide smaller pressure loss in total pressure than a normal shock.

3. Ejector's geometries and CFD model set up

In the simulation, the geometries of the calculation domain of the modeled steam ejectors were taken from those which were used in the experiment as described in Part 1. The ejector model consists of 4 parts which are the primary nozzle, the mixing chamber, the constant-area throat and the subsonic diffuser as shown in Fig. 2. The significant geometries of the primary nozzles, the mixing chambers and the throats were listed in Table 1.

Table 1
Ejector's geometry variation

Primary nozzle geometries			Mixing chamber inlet diameter		Throat length		
Nozzle No.	X	Y	Mixing chamber No.	Z	Throat No.	l	
	mm	mm		mm		mm	Times of diameter
1	2.00	8.00	1	24.00	1	19.00	1d
2	1.75	7.00	2	19.00	2	57.00	3d
3	1.50	6.00	3	29.00	3	95.00	5d
					4	114.00	6d

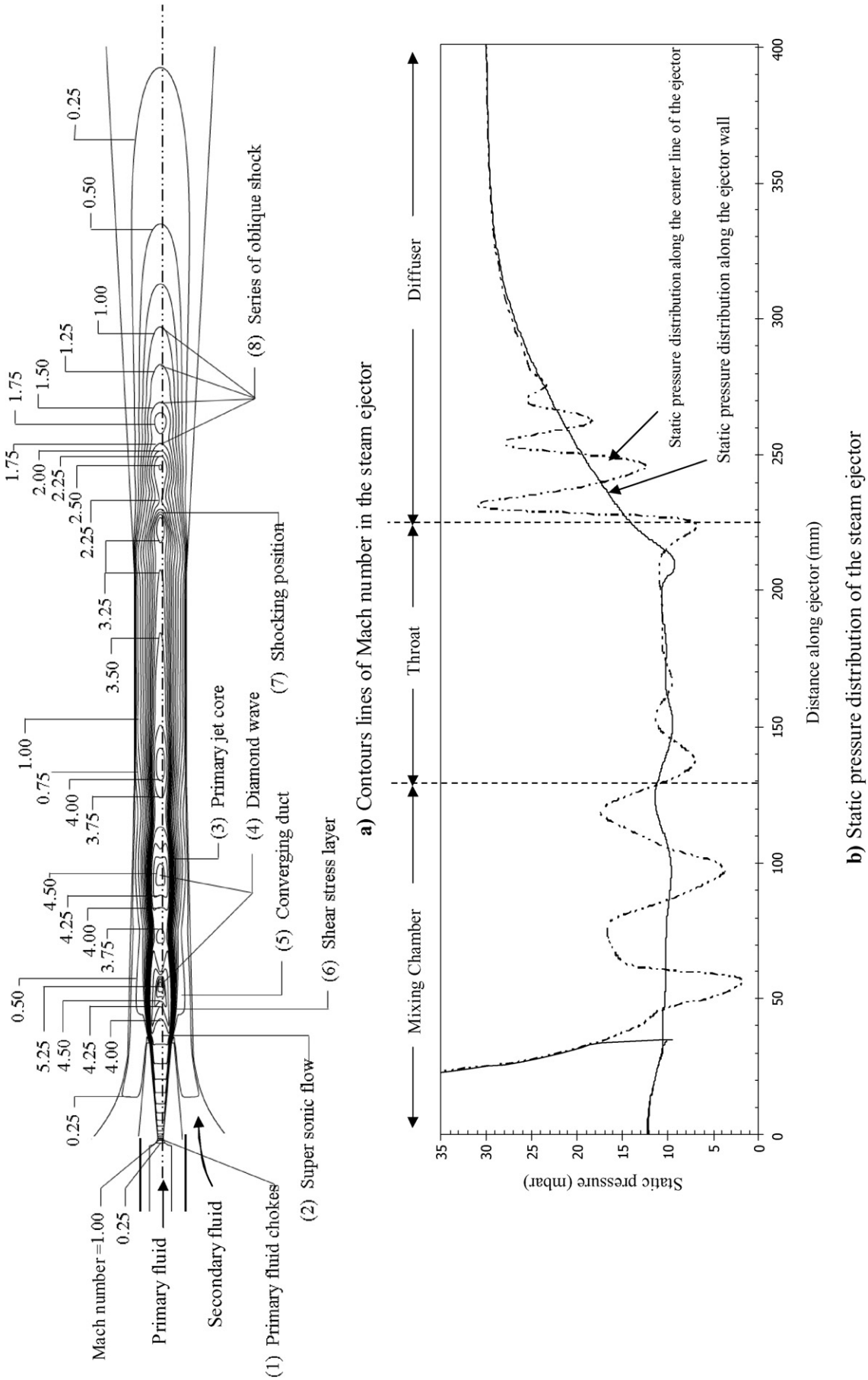

Fig. 1. Mach number and static pressure distribution in the steam ejector.

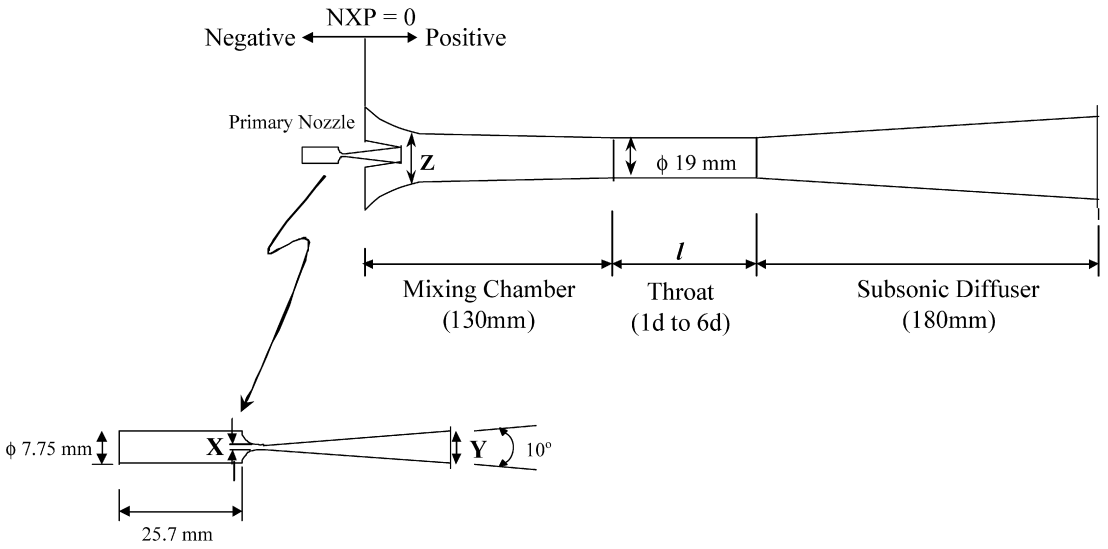

Fig. 2. Schematic diagram of the steam ejector.

Please note that in this study, the nozzle exit position (NXP) was kept constant at a positive distance of 35 mm. Every nozzle was modeled with the same area ratio, the nozzle exit to the throat. The diffuser was thought to have very small influence on ejector performance. Therefore, the studying of effect of the diffuser geometries was omitted and every test was done with the same diffuser. Details on the CFD model setup, grid generation, boundary conditions, working fluid properties were already explained in Part 1.

4. Effect of operating pressures

The investigations of the effects of operating pressures were carried out over a variety of upstream and downstream operating pressures. During the simulation, the primary fluid saturated temperature (boiler temperature, T_P) ranged from 120 to 140 °C, corresponding to absolute pressure of around 2000 to 3600 mbar. The secondary fluid saturated temperature (evaporator temperature, T_S) was varied in the range of 5 to 15 °C, corresponding to absolute pressure of around 8.5 to 17 mbar. Lastly, the back pressure (condenser pressure, P_C), the "*downstream of the ejector*", was varied from 30 to 60 mbar. To avoid any unwanted influences from other parameters, the studies were done with a fixed geometries ejector. The modeled ejector was constructed from primary nozzle No. 1, mixing chamber No. 1, throat section No. 3 and the subsonic diffuser.

Fig. 3 represents the calculated entrainment ratio when upstream and downstream pressures of the ejector were varied. At each setting of the primary fluid and secondary fluid condition, the operation of an ejector can be categorized into 3 regions, the choked flow, the un-choked flow and the reversed flow of secondary fluid as already discussed in Part 1 [1]. The ejector entrains the same amount of secondary fluid when it operates under critical back pressure. If the ejector operates beyond the critical point, the entrainment rate drops with an increasing of the downstream pressure.

Considering filled contours of Mach number simultaneously with static pressure profiles along the centerline of the steam

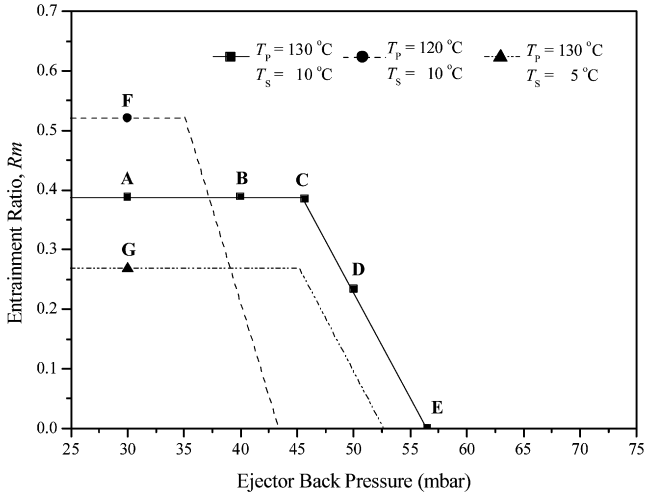

Fig. 3. Variation of calculated entrainment ratio of a steam ejector, effect of operating pressures.

ejector as shown in Figs. 4 and 5, increasing downstream pressure from **A** to **E** caused the shocking position to move upstream into the ejector throat. However, when a back pressure is not exceed the critical point or within the choked flow region (**A**, **B** and **C**), the shock will not affect the mixing behavior of the two streams. Flow structures in front of a shocking position are shown unchanged and the size of the primary jet core remained constant and independent from downstream conditions. It was thought, that during this choke flow region, the effective areas were always forced to appear within the constant area throat, since, the entrainment ratio remained constant. This proved the existence of the choking phenomenon.

When a downstream pressure increased higher than the critical point (**D** and **E**), the second series of oblique shocks was forced to move further upstream and combine with the first series of oblique shocks to form a single series of oblique shocks. This movement of the second series of oblique shocks caused the secondary fluid to be no longer choked, hence, disturbed

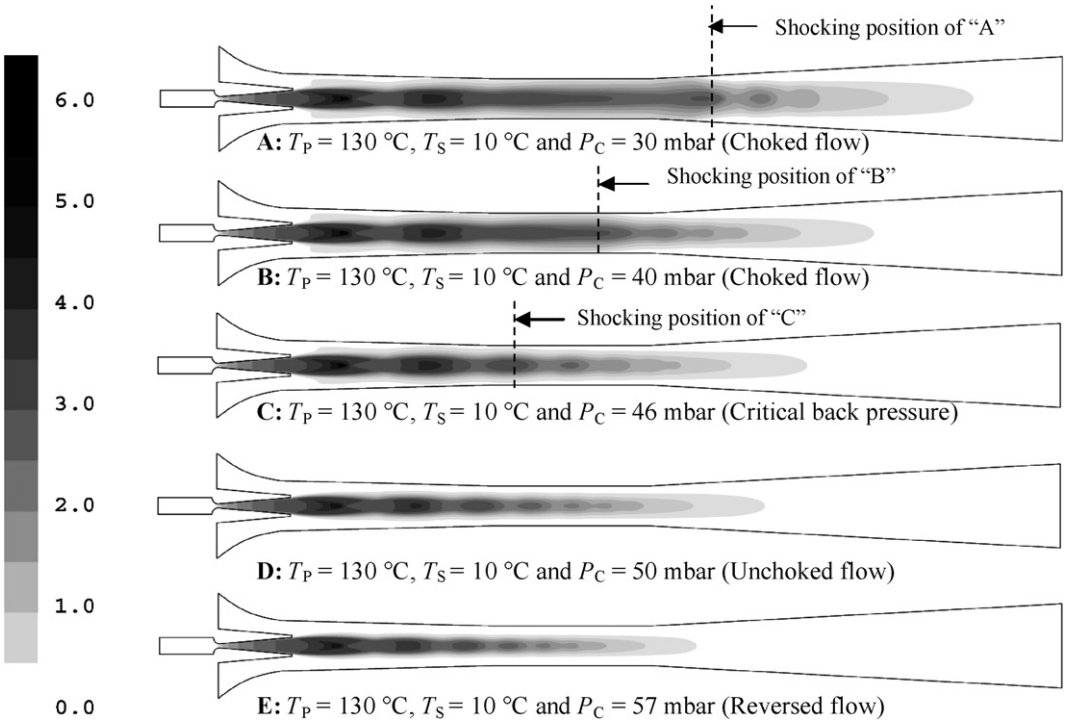

Fig. 4. Filled contours of Mach number: Effect of downstream pressure. (All operating points, **A**, **B**, **C**, **D**, and **E**, correspond to those shown in Fig. 3.)

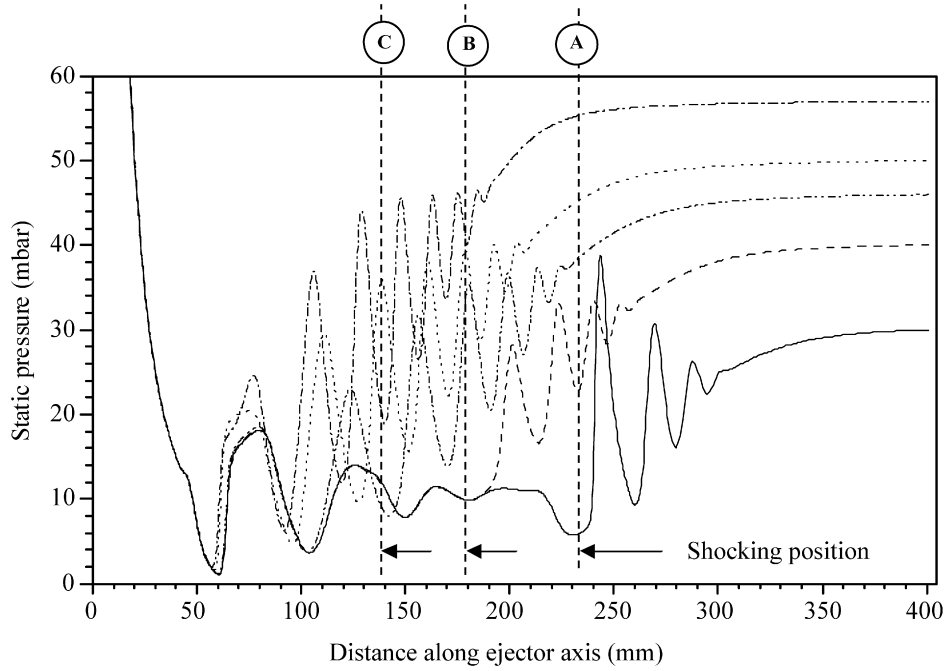

Fig. 5. Static pressure distribution along the centerline of the steam ejector: Effect of downstream pressure.

the entrainment process. This can be investigated from the lowering of an entrained fluid speed and hence, the increasing of static pressure before shock. It should be noted that the size and the momentum of the jet core was independent from the variation of downstream pressure.

Fig. 6 (**F** and **A**) shows that increasing the primary fluid pressure, the Mach number of motive fluid leaving a primary nozzle remains unchanged. This obeys the principle of supersonic compressible flow; the supersonic flow leaves the different converging-diverging nozzles at the same speed when those nozzles are modeled with the identical area ratios. However, the mass flow through the primary nozzle and the momentum of the flow were increased. The increasing of momentum allowed the primary fluid to leave and further under-expand and accelerate with larger expansion angle. This causes the diamond flow to shock at a higher Mach number at the first oblique shock as

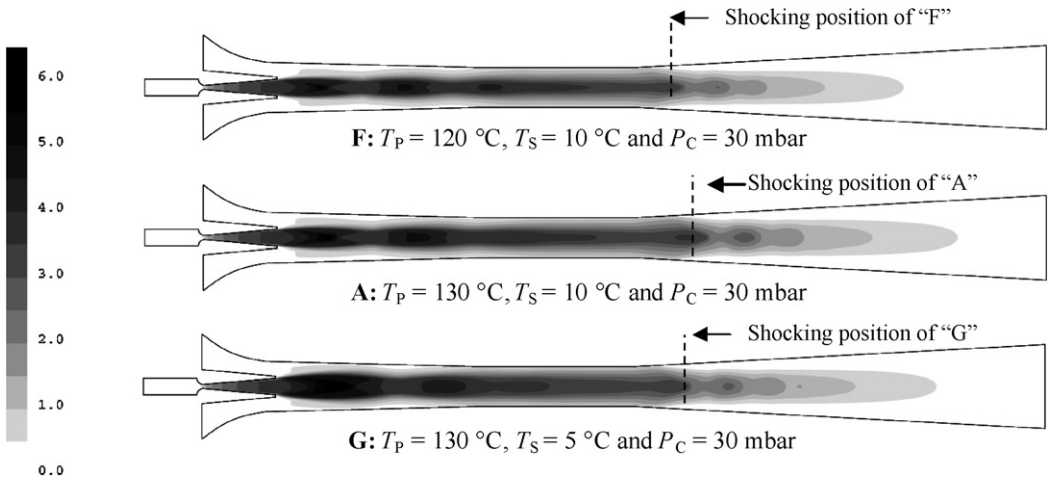

Fig. 6. Filled contours of Mach number: Effect of primary and secondary fluid saturated pressure. (All operating points, **A**, **F**, and **G**, correspond to those shown in Fig. 3.)

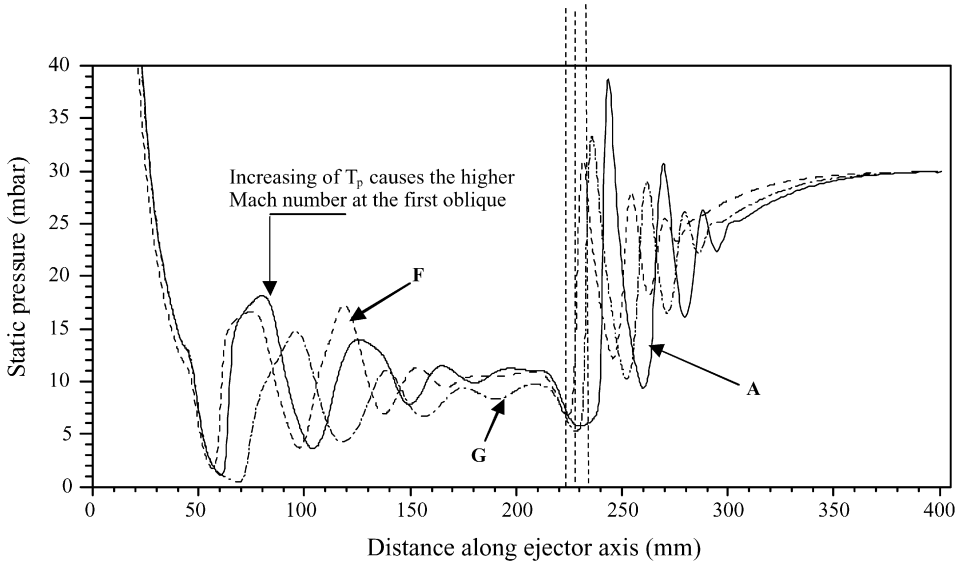

Fig. 7. Static pressure distribution along the centerline of the steam ejector: Effect of primary and secondary fluid saturated pressure.

can be seen in Fig. 7. The increased expansion angle causes the enlarging of a jet core, therefore, the annulus effective area is reduced and less secondary fluid can be entrained and accelerated through the steeper converging duct. However, with higher momentum of the jet core, the shocking position moves downstream, and the ejector can be operated at a higher discharged pressure.

When secondary fluid pressure is increased, it can be seen from the Mach number contours, Fig. 6 (**G** and **A**), that the expansion angle of under-expanded wave was influenced by an increasing of the secondary fluid pressure. The pressurized condition causes the lowering of expansion angle, thus smaller jet core and larger effective area result. The expanded wave was further accelerated at a lower Mach number. Therefore, momentum of the jet core was reduced. However, an enlarged effective area allows a larger amount of secondary fluid to be entrained and passed through the converging duct. Total momentum of the mixed stream which was decreased by the jet core is compensated by the higher secondary fluid pressure. So, it can be concluded that the total momentum of mixed stream becomes higher, and the shocking position moves downstream as the secondary fluid saturated pressure rises. This enables the ejector to be operated at higher downstream pressure.

5. Effect of ejector geometries

To study the effect of ejector geometries on the performance of the ejector, 3 interested parameters concerning the geometries were (1) the primary nozzle geometries, (2) the geometries of the mixing chamber, and (3) the geometries of the ejector's throat section. To investigate the influences of each parameter, the ejector was modeled with the different pieces of components. During the simulation, the upstream operating conditions were fixed, i.e., primary fluid saturated temperature of 130 °C and secondary fluid saturated temperature of 5 °C. Please also note that, the comparisons of flow structures in this section were made when the ejectors were operated at the choke flow

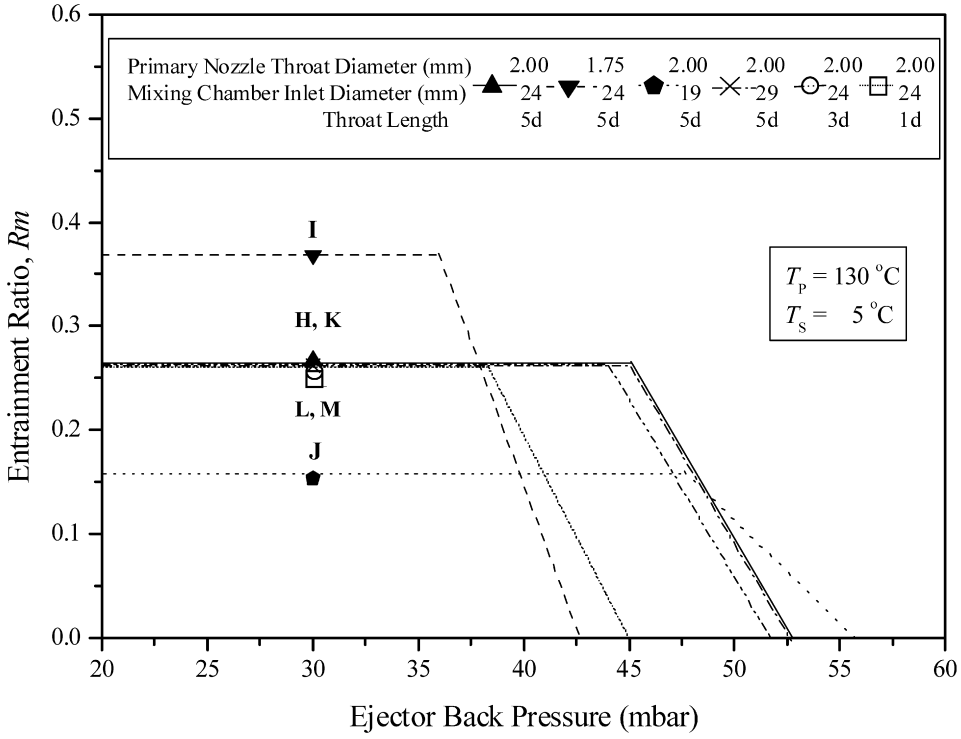

Fig. 8. Variation of calculated entrainment ratio of a steam ejector, effect of ejector geometries.

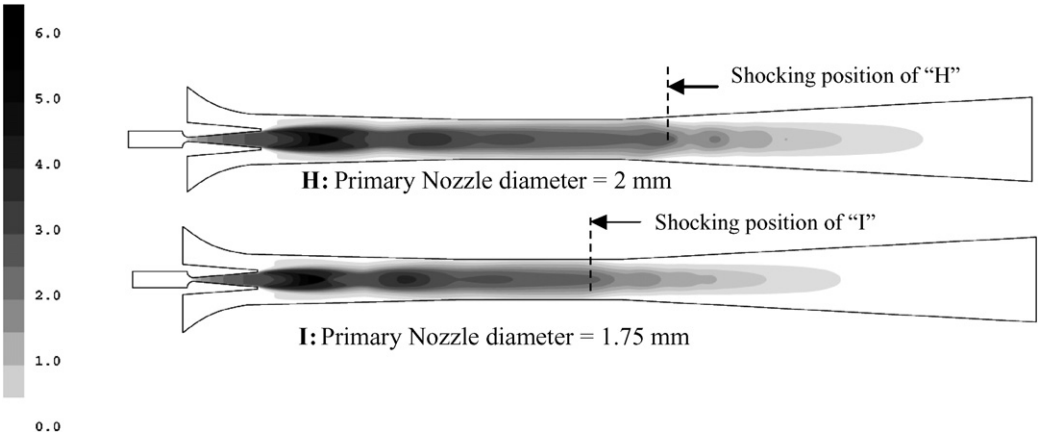

Fig. 9. Filled contours of Mach number: Effect of primary nozzle size. (All operating points, **H** and **I**, correspond to those shown in Fig. 8.)

mode or at the downstream pressure of 30 mbar as shown in Fig. 8.

From Fig. 8, point **I** and **H**, it is seen that when the ejector is equipped with a smaller primary nozzle (**I**), the entrainment ratio of the ejector can be increased. However, the ejector has to be operated at a lower critical back pressure.

Fig. 9 shows the contours of Mach number of a steam ejector, when its primary nozzle geometry is varied. When the ejector is equipped with a larger primary nozzle, a larger jet core which has higher momentum is produced. Therefore a smaller amount of the secondary fluid is allowed to be entrained through the resultant smaller effective area. On the other hand, the total momentum of the mixed stream increases and a stronger second series of oblique shock can be induced as seen in Fig. 10. Consequently, less compression process from the divergent diffuser is needed, and the shocking position moves forward closer to the ejector exit. In conclusion, these flow structures cause a decrease of the entrainment ratio. However, an ejector can be operated at a higher critical back pressure.

Fig. 11 demonstrates the contours of Mach number of a steam ejector, when its mixing chamber inlet diameter is varied. The investigations are made at a downstream pressure of 30 mbar. Obviously, when the ejector is assembled with the converging duct mixing type, **H** and **K**, the graphic flow visualization indicates that there is not much effect of the shear mixing and the viscosity of the fluid on the expanded wave. The primary jet core of the smaller entrance ejector moves with slightly greater speed and hence higher momentum. On the other hand, entraining the secondary fluid under a higher effect of the shear mixing and the viscosity of the fluid on

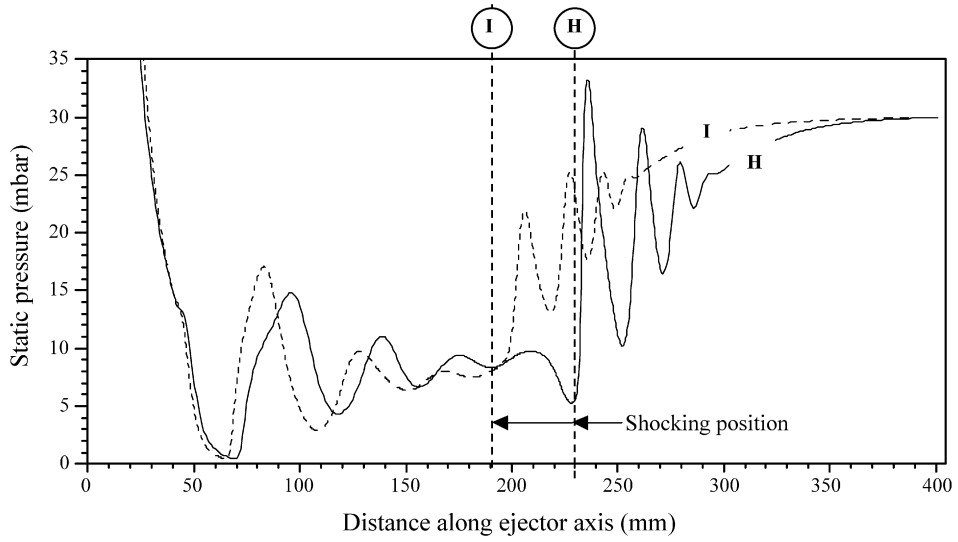

Fig. 10. Static pressure distribution along the centerline of the steam ejector: Effect of primary nozzle size.

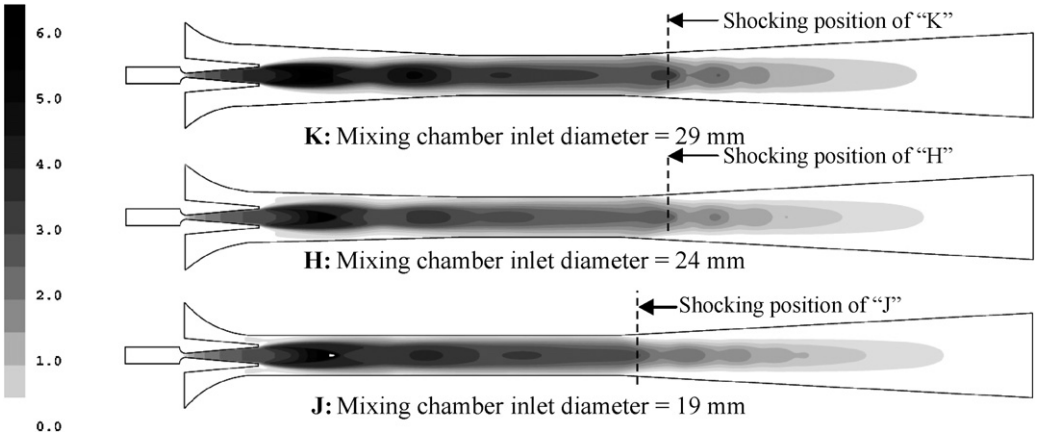

Fig. 11. Filled contours of Mach number: Effect of mixing chamber inlet diameter. (All operating points, **H**, **J** and **K**, correspond to those shown in Fig. 8.)

the expanded wave introduces the higher total pressure loss to the mixed stream. Therefore, it is investigated that the shocking position and the critical back pressure of both converging duct mixing ejectors are almost unchanged. Moreover, it is seen that the size of jet core and the effective area of both ejectors are similar. Therefore, they can draw the identical amount of secondary fluid, and their entrainment ratios remain the same.

Concerning the constant-area mixing ejector, **J**, the flow structures of this type of ejector are apparently different from the converging duct mixing ejector. The effect from the mixing chamber inlet is obvious. Less shear mixing and viscous effect in the mixing tube causes the expanded wave to leave the nozzle with a large expansion angle. A very large high speed primary jet core, and consequently a very small converging duct, is the result. Therefore, smaller amounts of the secondary fluid can be entrained through this converging duct, and the ejector has less entrainment ratio. Since the flow structures inside the constant-area mixing ejector are quite different from those of the converging duct mixing ejector; the position of the effective area is moved. Thus, the comparison between the shocking positions of two different types of ejector cannot be used to predict the trend of the critical condenser pressure.

Referring to Fig. 8, point **H**, **L** and **M** illustrate the performance characteristic of a steam ejector when its throat length was varied. It is clear that the length of the ejector throat section has almost no influence on the entrainment ratio of the ejector. However, when the ejector is assembled with a longer throat (**H**), the ejector can be operated at a higher critical back pressure.

Fig. 13 illustrates the graphic flow visualization inside the steam ejector, when the length of the ejector's throat section is varied. It is seen that the length of the ejector throat has almost no influence on the flow structure inside the steam ejector. These modeled ejectors show the identical sizes of the primary jet core, the expansion angle and resulted in the same size of the effective area. Therefore, the same amount of the secondary fluid can be drawn into the ejector, and consequently the entrainment ratio remains constant.

One interesting point is that the shape of the second series of oblique shock can vary with the length of ejector throat. It is thought that better mixing between the primary jet core and

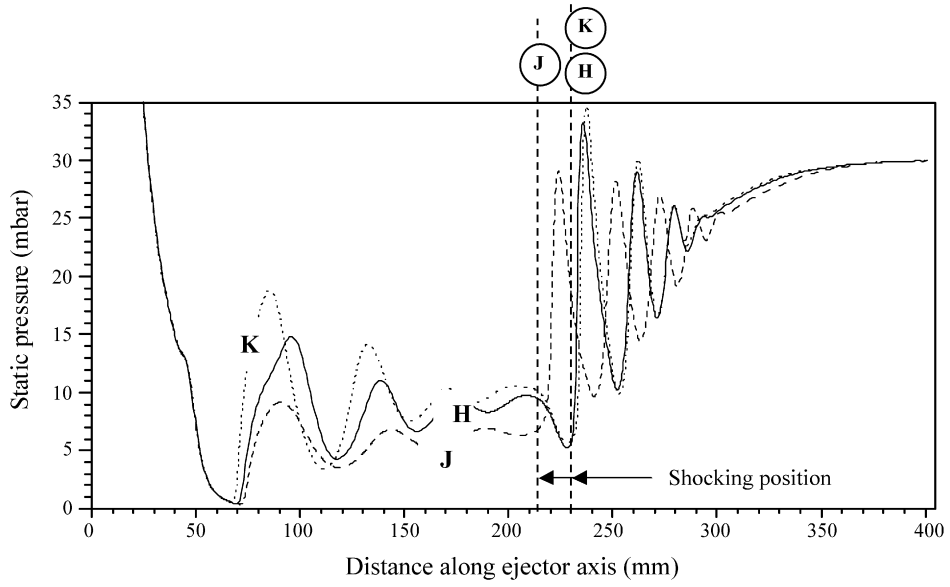

Fig. 12. Static pressure distribution along the centerline of the steam ejector: Effect of mixing chamber inlet diameter.

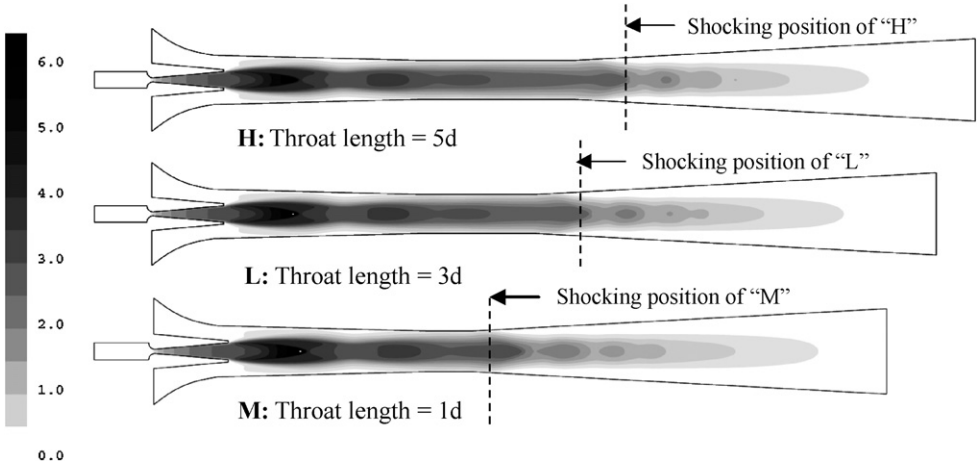

Fig. 13. Filled contours of Mach number: Effect of throat length. (All operating points, **H**, **L** and **M**, correspond to those shown in Fig. 8.)

the entrained fluid can be achieved when the longer contact time is provided, as the ejector is fitted with a longer throat section. The better mixing causes the smaller difference between the speed of the primary jet core and the surrounding secondary fluid. Thus the mixed stream becomes more uniform. The induced oblique shock is flattened and a higher compression effect across the shock wave can be achieved, as can be seen in Fig. 14. Therefore, less compression effect from the divergent portion of a subsonic diffuser is required, and the shocking position moves closer to the diffuser exit. In conclusion, the extended length of the throat section, plus the moving downstream of the shocking position provide a longer distance between the shocking position and the effective area. Therefore, the ejector can be operated at a higher critical back pressure.

However, please note that the elongation of the ejector throat introduces the pressure loss from the interaction of the flow with the viscous boundary layer on the ejector wall. In addition, the reduction of total pressure of the mixed stream is also a result of the induced stronger shock wave. Even though these losses are believed to be small, the accumulated losses from a very long throat and the very strong shock can mitigate the advantage of ejector throat length on the critical point of an ejector.

From the study, it is found that the location of the second shock wave can be varied between the end of the ejector throat and the beginning of the divergent portion of the diffuser. It is determined by the ejector operating conditions which affect the increase of static pressure across the shocking process, plus that in the divergent portion of the subsonic diffuser behind the process. Therefore, in some situation when the shocking position is created in the subsonic diffuser, the supersonic stream is first further accelerated, and its static pressure decreases. However, right after the first shock, its static pressure rebounds and rises to the discharge value.

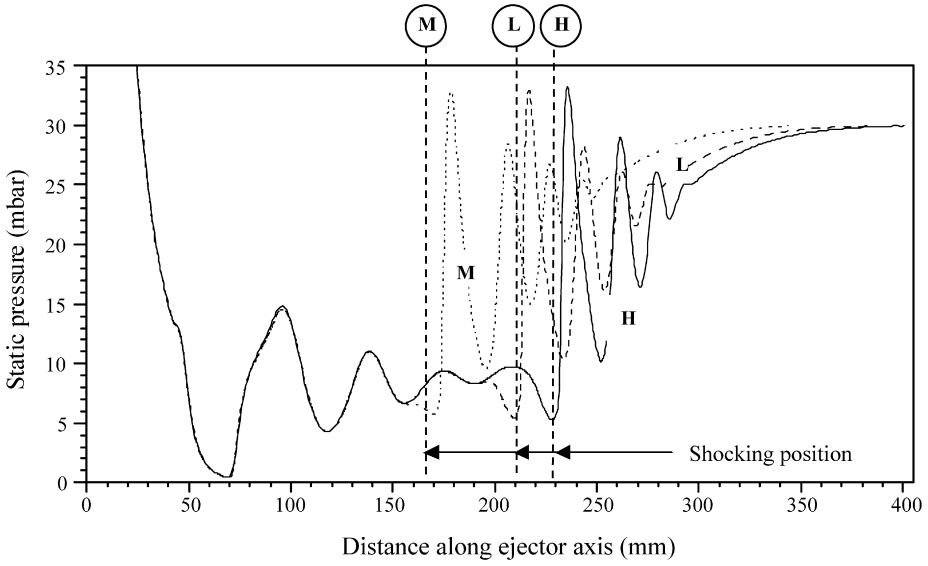

Fig. 14. Static pressure distribution along the centerline of the steam ejector: Effect of throat length.

6. Conclusion

In this paper, after the validation of the ejector's model was satisfied as described in Part 1 [1], the theory describing the flow and mixing process in the steam ejector is proposed. The static pressure distribution, the graphic flow visualization and other related flow information were used to explore the changes of flow structures and its behaviors inside the ejector conduit which caused the variation of its performances. With help of the CFD, the flow phenomena in the steam ejector are summarized as follows.

- The CFD visualization shows that the effective area as proposed by Huang [4] does exist; however, it is difficult to locate the exact position of the effective area within the ejector. In the choke flow mode, the entrainment ratios remained constant, the effective area, hence, can be estimated at anywhere within the constant area ejector's throat.
- Two series of oblique shocks were found in the simulation. The first series was found immediately after the primary fluid stream leaves the primary nozzle and begins to mix with the secondary fluid stream. The second series of oblique shock was found at the beginning of the diffuser section as a result of a non-uniform mixed stream. A major compression effect is caused by this second series of oblique shock. This latter shock is definitely contrary to a single normal shock which was proposed by Keenan's theory [5,6]. This is probably because this study utilized relative lower pressure of the primary fluid (boiler saturated temperature of 120–140 °C), while others used larger industrial boiler to produce the higher pressure primary fluid (boiler saturated temperature of 160–220 °C).

The influences of the studied parameters on the performance characteristic of a steam ejector are presented in Table 2.

From this table, it can be seen that both entrainment ratio and critical back pressure can be varied simultaneously by adjusting 3 parameters, which are (1) the primary fluid saturated pressure, (2) the secondary fluid saturated pressure, and (3) the primary nozzle size. However, when adjusting the primary fluid saturated pressure and primary nozzle size, the entrainment ratio and the critical back pressure cannot be increased together. The only adjustment which can increase both performance parameters simultaneously, the most desired condition, is the increase of the secondary fluid saturated temperature. Unfortunately, this achievement comes with the sacrifice of the refrigerated temperature.

The critical back pressure of a steam ejector can be increased by using an ejector with a longer throat section. As described previously, the elongation of the ejector throat has no influence

Table 2
Effect of operating pressures and ejector's geometries on the performance of steam ejector

Parameter	Action	Performance characteristic	
		Entrainmentratio (Rm)	Critical backpressure (P_c)
Ejector operating pressures			
Primary fluid saturated pressure	↑	↓	↑
Secondary fluid saturated pressure	↑	↑	↑
Ejector geometries			
Primary nozzle size	↑	↓	↑
Mixing chamber inlet diameter	↑	–	Unpredictable
Ejector throat length	↑	–	↑

on its entrainment ratio; however, if the throat section is too long, the loss in total pressure may mitigate its advantage on the back pressure which the mixed stream can emit.

In conclusion, this study shows the proficiency of CFD in predicting the performance of the ejector, both entrainment ratio and critical back pressure. It also provides a good explanation of the flow structure in the ejector. Using the information obtained from the CFD leads to the development in the design of high performance ejector.

Acknowledgements

The research was financed by Thailand Research Fund. The first author would like to thank the Royal Golden Jubilee Program, Government of Thailand for his academic sponsorship.

References

[1] T. Sriveerakul, et al., Performance prediction of steam ejector using computational fluid dynamics: Part 1. Validation of the CFD results, Internat. J. Thermal Sci. (2006), doi: 10.1016/j.ijthermalsci.2006.10.014.
[2] J.D. Anderson, Modern Compressible Flow, with Historical Perspective, third ed., McGraw-Hill, 2002.
[3] J.T. Munday, D.F. Bagster, A new theory applied to steam jet refrigeration, Ind. Engrg. Chem. Process Des. Dev. 16 (4) (1977) 442–449.
[4] B.J. Huang, C.B. Jiang, F.L. Hu, Ejector performance characteristics and design analysis of jet refrigeration system, Trans. ASME 107 (1985) 792–802.
[5] J.H. Keenan, E.P. Neumann, F. Lustwerk, An investigation of ejector design by analysis and experiment, ASME J. Appl. Mech. 72 (1950) 299–309.
[6] J.H. Keenan, E.P. Neumann, A simple air ejector, ASME J. Appl. Mech. 64 (1942) 75–81.